Mediterr. J. Math. (2025) 22:77
https://doi.org/10.1007/s00009-025-02841-2
1660-5446/25/030001-17
*published online* April 24, 2025


Mediterranean Journal of Mathematics



# Covers of Fractal Interpolation Surfaces with Finite Families of Octahedrons

Bogdan-Cristian Anghelina and Radu Miculescu

**Abstract.** In a previous work (Chaos Solitons Fract 173:113674, 2023), we presented a method for finding a finite family of closed balls whose union contains the attractor of a given iterated function system. In this paper, for the particular framework of fractal interpolation surfaces, we provide an improved version of it. This approach is more efficient, from the computational point of view, as it is based on finding the maximum of certain sets, in contrast to the previous method which uses a sorting algorithm.

**Mathematics Subject Classification.** 28A80, 41A05, 26A16, 26A18.

**Keywords.** Iterated function systems, fractal interpolation surfaces, octahedrons, covers.

## 1. Introduction

Iterated function systems were first introduced by Hutchinson [17] and later gained prominence through the work of M. Barnsley. These systems are defined as pairs $\mathcal{S} := ((X, d), (f_i)_{i\in I})$, where $(X, d)$ is a complete metric space, $I$ is a nonempty finite index set, and each function $f_i : X \to X$ is a contraction.

A key concept associated with iterated function systems is the fractal operator, $F_{\mathcal{S}} : P_{cp}(X) \to P_{cp}(X)$, given by

$$F_{\mathcal{S}}(K) = \bigcup_{i\in I} f_i(K),$$

for all $K \in P_{cp}(X)$, where $P_{cp}(X)$ represents the collection of all nonempty compact subsets of $X$. It can be shown that, with respect to the Hausdorff–Pompeiu metric $h$, this operator is a contraction. Since $(P_{cp}(X), h)$ is a complete metric space, the Banach fixed-point theorem ensures the existence of a unique fixed point, referred to as the attractor of the system, denoted by $A_{\mathcal{S}}$.

Barnsley used the framework of iterated function systems to initiate the theory of fractal interpolation functions, a method for constructing continuous functions that interpolate given data while exhibiting fractal-like properties. Given a dataset of $N+1$ points

$$\{(x_i, y_i) \mid i \in \{0, 1, \ldots, N\}\} \subseteq [x_0, x_N] \times \mathbb{R},$$

this approach generates a continuous function $f : [x_0, x_N] \to \mathbb{R}$ that satisfies

$$f(x_i) = y_i,$$

for all $i$, while ensuring that its graph is the attractor of a carefully designed iterated function system. This method is particularly well suited for modeling irregular and complex curves and surfaces, with applications spanning computer graphics, metallurgy, geology, and seismology. Further details can be found in [2], along with generalizations in [3,4].

Fractal interpolation has also been extended to surfaces. Massopust [22] developed an approach for constructing fractal interpolation surfaces over triangular regions, assuming that the interpolation points along the boundary lie in a common plane. Further related results are discussed in [19]. Geronimo and Hardin [15] proposed algorithms for generating fractal interpolation surfaces over arbitrary polygonal regions, allowing interpolation at unrestricted points; a broader generalization of this work can be found in [36]. In a different direction, Hardin and Massopust [16] explored multivariable fractal functions in $\mathbb{R}^m$. Other notable contributions include the work of Dalla [11], as well as Xie and Sun [32], who constructed bivariate fractal interpolation functions over rectangular domains in $\mathbb{R}^2$, where interpolation points along each edge are collinear. These ideas have been further developed in [13,21].

An alternative construction for fractal interpolation surfaces, based on fractal interpolation functions, is presented in [6], with further generalizations in [35]. Additional works exploring generalizations of fractal interpolation surfaces can be found in [4,5,9,10,12,14,18,20,23–31]. These methods have found numerous practical applications, including surface approximation in geology and materials science [33], terrain modeling [34], planetary surface reconstruction [8], and image compression [7].

A crucial aspect of working with iterated function systems involves estimating the attractor's structure. In [1], we proposed a method for constructing a finite collection of closed balls whose union contains the attractor, a result particularly useful in approximating its box-counting dimension. More precisely, given an iterated function system $\mathcal{S} = ((X, d), (f_i)_{i\in I})$ with at least two functions, we considered $\rho_i \in [0, \infty)$, $i \in I$, satisfying

$$(*) \qquad \rho_i = \mathrm{Lip}(f_i)\left(\max_{i,j\in I} d(e_i, e_j) + \max_{j\in I\setminus\{i\}} \rho_j\right),$$

where $e_i$ is the unique fixed point of $f_i$ and $\mathrm{Lip}(f_i)$ is its Lipschitz constant. In this case, the attractor $A_{\mathcal{S}}$ is contained within $\bigcup_{i\in I} B[e_i, \rho_i]$.

To find a solution of $(*)$, we initially relabeled the functions $f_i$ in increasing order of their Lipschitz constants, a computationally inefficient approach.

In this paper, we refine this method and adapt it to the specific context of fractal interpolation surfaces. A primary challenge in this setting is determining explicit values for $\mathrm{Lip}(f_i)$ from the given data. However, following the approach in [11], one can find some constants $c_i \in [0,1)$ such that

$$d(f_i(x), f_i(y)) \leq c_i d(x,y), \quad \forall x, y \in X.$$

By substituting $\mathrm{Lip}(f_i)$ with these constants $c_i$, we preserve the validity of our previous results while improving computational efficiency. Rather than ordering the Lipschitz constants, we propose a more direct approach by identifying $\max_{i\in I} c_i$ and $\max_{j\in I, c_j \neq \max_{i\in I} c_i} c_j$. This alternative method eliminates unnecessary computations while ensuring accuracy in estimating the attractor's structure. The paper also presents graphical representations that illustrate these covers for fractal interpolation surfaces.

By refining existing techniques and introducing a more computationally efficient approach, this work contributes to the broader study of fractal interpolation, providing new insights into the approximation and visualization of complex surfaces.

## 2. Preliminaries

### 2.1. Notation and Basic Definitions

Given a metric space $(X,d)$, $x \in X$ and $r > 0$ we shall use the following notation:

- $B[x,r] = \{y \in X \mid d(y,x) \leq r\}$
- $P_{cp}(X) = \{A \subseteq X | A \text{ is non-empty and compact}\}$
- $h$ is the Hausdorff–Pompeiu metric.

For a Lipschitz function $f : X \to X$ we shall denote by $\mathrm{Lip}(f)$ the Lipschitz constant of $f$.

**Definition 2.1.** An iterated function system (for short IFS) is a pair $\mathcal{S} = \big((X,d),(f_i)_{i\in I}\big)$, where $(X,d)$ is a complete metric space and $f_i : X \to X$, $i \in I$, are Banach contractions.

The function $F_{\mathcal{S}} : P_{cp}(X) \to P_{cp}(X)$, given by

$$F_{\mathcal{S}}(K) = \bigcup_{i\in I} f_i(K),$$

for every $K \in P_{cp}(X)$, is called the fractal operator (or the Hutchinson operator) associated with $\mathcal{S}$.

**Proposition 2.1.** *If $\mathcal{S} = \big((X,d),(f_i)_{i\in I}\big)$ is an iterated function system, then $F_{\mathcal{S}}$ is a contraction with respect to $h$. Its unique fixed point is denoted by $\mathcal{A}_{\mathcal{S}}$ and it is called the attractor of $\mathcal{S}$ since*

$$\lim_{n\to\infty} \underbrace{(F_{\mathcal{S}} \circ F_{\mathcal{S}} \circ \cdots \circ F_{\mathcal{S}})}_{n \text{ times}}(K) = \mathcal{A}_{\mathcal{S}},$$

*for each $K \in P_{cp}(X)$.*

### 2.2. Fractal Interpolation Surfaces

In this section, following [11], we present the basic facts concerning fractal interpolation surfaces.

Let $I = [a, b], J = [c, d]$ and the data set $\mathcal{D} = \{(x_k, y_l, z_{k,l}) \in \mathbb{R}^3 | k \in \{0, 1, \ldots, n\}, l \in \{0, 1, \ldots, m\}\}$ be such that

$$a = x_0 < x_1 < \cdots < x_{n-1} < x_n = b,$$
$$c = y_0 < y_1 < \cdots < y_{m-1} < y_m = d,$$

and each of the sets

$$(**) \qquad \begin{array}{l} \{(x_0, y_l, z_{0,l}) | l \in \{0, 1, \ldots, m\}\}, \\ \{(x_n, y_l, z_{n,l}) | l \in \{0, 1, \ldots, m\}\}, \\ \{(x_k, y_0, z_{k,0}) | k \in \{0, 1, \ldots, n\}\}, \\ \{(x_k, y_m, z_{k,m}) | k \in \{0, 1, \ldots, n\}\} \end{array}$$

consists of collinear points.

For $k \in \{1, \ldots, n\}$ and $l \in \{1, \ldots, m\}$ we define the function $F_{k,l} : I \times J \times \mathbb{R} \to I \times J \times \mathbb{R}$, by

$$F_{k,l}(x, y, z) = (a_k x + b_k, c_l y + d_l, e_{k,l} x + f_{k,l} y + g_{k,l} z + \alpha_{k,l} xy + \beta_{k,l}),$$

for all $(x, y, z) \in I \times J \times \mathbb{R}$, where the coefficients $a_k, b_k, c_l, d_l, e_{k,l}, f_{k,l}, g_{k,l}, \alpha_{k,l}$ and $\beta_{k,l}$ are chosen such that

$$F_{k,l}(x_0, y_0, z_{0,0}) = (x_{k-1}, y_{l-1}, z_{k-1,l-1}),$$
$$F_{k,l}(x_n, y_0, z_{n,0}) = (x_k, y_{l-1}, z_{k,l-1}),$$
$$F_{k,l}(x_0, y_m, z_{0,m}) = (x_{k-1}, y_l, z_{k-1,l})$$

and

$$F_{k,l}(x_n, y_m, z_{n,m}) = (x_k, y_l, z_{k,l}).$$

Equivalently, we obtain the following systems of equations

$$\begin{cases} a_k x_0 + b_k & = x_{k-1} \\ c_l y_0 + d_l & = y_{l-1} \\ e_{k,l} x_0 + f_{k,l} y_0 + g_{k,l} z_{0,0} + \alpha_{k,l} x_0 y_0 + \beta_{k,l} & = z_{k-1,l-1} \end{cases},$$

$$\begin{cases} a_k x_n + b_k & = x_k \\ c_l y_0 + d_l & = y_{l-1} \\ e_{k,l} x_n + f_{k,l} y_0 + g_{k,l} z_{n,0} + \alpha_{k,l} x_n y_0 + \beta_{k,l} & = z_{k,l-1} \end{cases},$$

$$\begin{cases} a_k x_0 + b_k & = x_{k-1} \\ c_l y_m + d_l & = y_l \\ e_{k,l} x_0 + f_{k,l} y_m + g_{k,l} z_{0,m} + \alpha_{kl} x_0 y_m + \beta_{k,l} & = z_{k-1,l} \end{cases}$$

and

$$\begin{cases} a_k x_n + b_k & = x_k \\ c_l y_m + d_l & = y_l \\ e_{k,l} x_n + f_{k,l} y_m + g_{k,l} z_{n,m} + \alpha_{k,l} x_n y_m + \beta_{k,l} & = z_{k,l} \end{cases}.$$

From the first two equations of each system we obtain

$$a_k = \frac{x_k - x_{k-1}}{x_n - x_0},\ b_k = \frac{x_{k-1}x_n - x_k x_0}{x_n - x_0},\ c_l = \frac{y_l - y_{l-1}}{y_m - y_0} \text{ and } d_l = \frac{y_{l-1}y_m - y_l y_0}{y_m - y_0}.$$

From the remaining equations we find

$$\begin{cases} e_{k,l}x_n + f_{k,l}y_m + g_{k,l}z_{n,m} + \alpha_{k,l}x_n y_m + \beta_{k,l} &= z_{k,l} \\ e_{k,l}x_0 + f_{k,l}y_m + g_{k,l}z_{0,m} + \alpha_{k,l}x_0 y_m + \beta_{k,l} &= z_{k-1,l} \\ e_{k,l}x_n + f_{k,l}y_0 + g_{k,l}z_{n,0} + \alpha_{k,l}x_n y_0 + \beta_{k,l} &= z_{k,l-1} \\ e_{k,l}x_0 + f_{k,l}y_0 + g_{k,l}z_{0,0} + \alpha_{k,l}x_0 y_0 + \beta_{k,l} &= z_{k-1,l-1} \end{cases}$$

and, with the notation

$$\begin{aligned} &p_{k,l} = z_{k,l} - g_{k,l}z_{n,m},\ q_{k,l} = z_{k-1,l} - g_{k,l}z_{0,m}, \\ &r_{k,l} = z_{k,l-1} - g_{k,l}z_{n,0} \text{ and } t_{k,l} = z_{k-1,l-1} - g_{k,l}z_{0,0}, \end{aligned}$$

we get

$$\begin{cases} e_{k,l}x_n + f_{k,l}y_m + \alpha_{k,l}x_n y_m + \beta_{k,l} &= p_{k,l} \\ e_{k,l}x_0 + f_{k,l}y_m + \alpha_{k,l}x_0 y_m + \beta_{k,l} &= q_{k,l} \\ e_{k,l}x_n + f_{k,l}y_0 + \alpha_{k,l}x_n y_0 + \beta_{k,l} &= r_{k,l} \\ e_{k,l}x_0 + f_{k,l}y_0 + \alpha_{k,l}x_0 y_0 + \beta_{k,l} &= t_{k,l} \end{cases}.$$

Hence,

$$\begin{cases} e_{k,l} + \alpha_{k,l}y_m &= \frac{p_{k,l}-q_{k,l}}{x_n - x_0} \\ e_{k,l} + \alpha_{k,l}y_0 &= \frac{r_{k,l}-t_{k,l}}{x_n - x_0} \end{cases} \text{ and } \begin{cases} f_{k,l} + \alpha_{k,l}x_n &= \frac{p_{k,l}-r_{k,l}}{y_m - y_0} \\ f_{k,l} + \alpha_{k,l}x_0 &= \frac{q_{k,l}-t_{k,l}}{y_m - y_0} \end{cases}.$$

Therefore, for $g_{k,l}$ arbitrarily chosen in $(0,1)$, we have

$$\begin{aligned} \alpha_{k,l} &= \frac{p_{k,l} - q_{k,l} - r_{k,l} + t_{k,l}}{(x_n - x_0)(y_m - y_0)}, \\ e_{k,l} &= \frac{y_0(q_{k,l} - p_{k,l}) - y_m(t_{k,l} - r_{k,l})}{(x_n - x_0)(y_m - y_0)}, \\ f_{k,l} &= \frac{x_0(r_{k,l} - p_{k,l}) - x_n(t_{k,l} - q_{k,l})}{(x_n - x_0)(y_m - y_0)} \end{aligned}$$

and

$$\beta_{k,l} = \frac{y_0(x_0 p_{k,l} - x_n q_{k,l}) - y_m(x_0 r_{k,l} - x_n t_{k,l})}{(x_n - x_0)(y_m - y_0)}.$$

Furthermore, we define $\delta := \max\{|a|, |b|, |c|, |d|\}$ and $\theta = \min\{\theta_1, \theta_2\}$, where

$$\theta_1 = \begin{cases} 1, & \begin{matrix} e_{1,1} = \cdots = e_{n,m} = 0 \\ \alpha_{1,1} = \cdots = \alpha_{n,m} = 0 \end{matrix} \\ \dfrac{1 - \max\limits_{k\in\{1,\ldots,n\}} a_k}{2 \max\limits_{\substack{k\in\{1,\ldots,n\} \\ l\in\{1,\ldots,m\}}} (|e_{k,l}| + \delta|\alpha_{k,l}|)}, & \text{otherwise} \end{cases}$$

and

$$\theta_2 = \begin{cases} 1, & \begin{array}{l} f_{1,1} = \cdots = f_{n,m} = 0 \\ \alpha_{1,1} = \cdots = \alpha_{n,m} = 0 \end{array} \\ \dfrac{1 - \max\limits_{l\in\{1,\ldots,m\}} c_l}{2 \max\limits_{\substack{k\in\{1,\ldots,n\} \\ l\in\{1,\ldots,m\}}} (|f_{k,l}| + \delta|\alpha_{k,l}|)}, & \text{otherwise.} \end{cases}$$

On $\mathbb{R}^3 \times \mathbb{R}^3$ we define the metric $\rho : \mathbb{R}^3 \times \mathbb{R}^3 \to [0, \infty)$, given by

$$\rho((x, y, z), (x', y', z')) = |x - x'| + |y - y'| + \theta|z - z'|,$$

for all $(x, y, z), (x', y', z') \in \mathbb{R}^3$.

With these preparations we can show the following:

**Lemma 2.1.** *$F_{k,l}$ is a contraction with respect to $\rho$ for all $k \in \{1, \ldots, n\}$ and $\ell \in \{1, \ldots, m\}$.*

*Proof.* For $k \in \{1, \ldots, n\}$ and $\ell \in \{1, \ldots, m\}$ arbitrarily chosen, but fixed, we have

$$\begin{aligned} \rho(F_{k,l}(x, y, z), F_{k,l}(x', y', z')) &= a_k|x - x'| + c_l|y - y'| \\ &\quad + \theta|e_{k,l}(x - x') + f_{k,l}(y - y') + g_{k,l}(z - z') + \alpha_{k,l}(xy - x'y')| \\ &\leq (a_k + \theta|e_{k,l}|)|x - x'| + (c_l + \theta|f_{k,l}|)|y - y'| \\ &\quad + \theta g_{k,l}|z - z'| + \theta|\alpha_{k,l}||x(y - y') + y'(x - x')| \\ &\leq [a_k + \theta(|e_{k,l}| + \delta|\alpha_{k,l}|)]|x - x'| \\ &\quad + [c_l + \theta(|f_{k,l}| + \delta|\alpha_{k,l}|)]|y - y'| + \theta g_{k,l}|z - z'| \\ &\leq C_{k,l}\rho((x, y, z), (x', y', z')), \end{aligned}$$

for all $(x, y, z), (x', y', z') \in I \times J \times \mathbb{R}$, where

$$C_{k,l} = \max\{a_k + \theta(|e_{k,l}| + \delta|\alpha_{k,l}|),\ c_l + \theta(|f_{k,l}| + \delta|\alpha_{k,l}|),\ g_{k,l}\} < 1.$$

□

**Theorem 2.1** (Proposition 2.2 from [11]). *There exists a continuous function $f : I \times J \to \mathbb{R}$ having the following two properties:*

1. *For all $k \in \{0, 1, \ldots, n\}$ and $l \in \{0, 1, \ldots, m\}$*
$$f(x_k, y_l) = z_{k,l},$$
*i.e. $f$ interpolates $\mathcal{D}$.*
2. *If $\mathscr{S}$ is the IFS $((I \times J \times \mathbb{R}, \rho), (F_{k,l})_{k\in\{1,\ldots,n\},l\in\{1,\ldots,m\}})$, then*
$$G_f = \mathcal{A}_{\mathscr{S}}.$$

Note that, in view of Sect. 2.2, from [11], the collinearity condition (**) is not restrictive.

## 3. Main Results

We shall first show that the results from [1] remain valid under a broader assumption.

### 3.1. Covers with a Finite Family of Closed Balls of the Attractor of an IFS

In the sequel, we consider

- $\mathcal{S} = ((X, d), (f_i)_{i\in\{1,\dots,n\}})$ an iterated function system consisting of contractions, with $n \geq 2$
- $\gamma_i$ the unique fixed point of $f_i$, where $i \in \{1, \dots, n\}$
- $c_i \in [0, 1)$ such that $d(f_i(x), f_i(x)) \leq c_i d(x, y)$ for all $x, y \in X$, where $i \in \{1, \dots, n\}$
- $i' \in \{1, \dots, n\}$ such that $c_{i'} = \max\{c_1, \dots, c_n\}$
- $i'' \in \{1, \dots, n\} \setminus \{i'\}$ such that $c_{i''} = \max\{c_i \mid i \in \{1, \dots, n\}\setminus\{i'\}\}$
- $M = \max_{i,j\in\{1,\dots,n\}} d(\gamma_i, \gamma_j)$.
- The system $\mathfrak{S}$, with the unknowns $\rho_1, \dots \rho_n$, consisting on the following $n$ equations:

$$\rho_i = c_i \left( M + \max_{j\in\{1,\dots,n\}\setminus\{i\}} \rho_j \right),$$

where $i \in \{1, \dots, n\}$.

The reasoning behind Proposition 3.3 from [1] guarantees the validity of the following result:

**Proposition 3.1.** *Within the given framework, the attractor satisfies*

$$\mathcal{A}_{\mathcal{S}} \subseteq \bigcup_{i\in\{1,\dots,n\}} B[\gamma_i, \rho_i],$$

*for any solution $\rho_1, \dots, \rho_n$ of the system $\mathfrak{S}$.*

**Proposition 3.2.** *Under the same framework, the values*

$$\rho_{i'} = M c_{i'} \frac{1 + c_{i''}}{1 - c_{i'} c_{i''}}$$

*and*

$$\rho_i = M c_i \frac{1 + c_{i'}}{1 - c_{i'} c_{i''}},$$

*for all $i \in \{1, \dots, n\} \setminus \{i'\}$, constitute a solution of the system $\mathfrak{S}$.*

*Proof.* We begin by establishing the following claim
**Claim.**

$$\rho_{i'} \geq \rho_{i''} \geq \rho_i,$$

for all $i \in \{1, \dots, n\} \setminus \{i'\}$.

Justification of the Claim. We have

$$c_{i''}(1 + c_{i'}) = c_{i''} + c_{i'} c_{i''} \leq c_{i'} + c_{i'} c_{i''} = c_{i'}(1 + c_{i''}),$$

so

$$\rho_{i''} = M c_{i''} \frac{1 + c_{i'}}{1 - c_{i'} c_{i''}} \leq M c_{i'} \frac{1 + c_{i''}}{1 - c_{i'} c_{i''}} = \rho_{i'}.$$

Since $c_{i''} \geq c_i$ for all $i \in \{1, \dots, n\}\setminus\{i'\}$, we have

$$\rho_i = M c_i \frac{1 + c_{i'}}{1 - c_{i'} c_{i''}} \leq M c_{i''} \frac{1 + c_{i'}}{1 - c_{i'} c_{i''}} = \rho_{i''},$$

for all $i \in \{1,\dots,n\} \setminus \{i'\}$. Hence, the proof of the Claim is complete.

Therefore

$$\max_{j\in\{1,\dots,n\}\setminus\{i'\}} \rho_j = \rho_{i''}. \tag{1}$$

and

$$\max_{j\in\{1,\dots,n\}\setminus\{i\}} \rho_j = \rho_{i'}, \tag{2}$$

for all $i \in \{1,\dots,n\} \setminus \{i'\}$.

We have

$$\rho_{i'} = Mc_{i'}\frac{1+c_{i''}}{1-c_{i'}c_{i''}} = Mc_{i'}\frac{1-c_{i'}c_{i''}+c_{i'}c_{i''}+c_{i''}}{1-c_{i'}c_{i''}}$$
$$= c_{i'}\left(M + Mc_{i''}\frac{1+c_{i'}}{1-c_{i'}c_{i''}}\right) = c_{i'}\left(M+\rho_{i''}\right) \overset{(1)}{=} c_{i'}\left(M + \max_{j\in\{1,\dots,n\}\setminus\{i'\}}\rho_j\right)$$

and

$$\rho_i = Mc_i\frac{1+c_{i'}}{1-c_{i'}c_{i''}} = Mc_i\frac{1-c_{i'}c_{i''}+c_{i'}c_{i''}+c_{i'}}{1-c_{i'}c_{i''}}$$
$$= c_i\left(M + Mc_{i'}\frac{1+c_{i''}}{1-c_{i'}c_{i''}}\right) = c_i(M+\rho_{i'}) \overset{(2)}{=} c_i\left(M + \max_{j\in\{1,\dots,n\}\setminus\{i\}}\rho_j\right),$$

for all $i \in \{1,\dots,n\} \setminus \{i'\}$.

Thus, the given values of $\rho_i$ provide a solution of the system $\mathfrak{S}$, completing the proof. □

Combining Propositions 3.1 and 3.2, we establish the following theorem:

**Theorem 3.1.** *Under the given framework, the attractor satisfies*

$$\mathcal{A}_{\mathcal{S}} \subseteq \left(\bigcup_{i\in\{1,\dots,n\}\setminus\{i'\}} B\left[\gamma_i, Mc_i\frac{1+c_{i'}}{1-c_{i'}c_{i''}}\right]\right)\bigcup B\left[\gamma_{i'}, Mc_{i'}\frac{1+c_{i''}}{1-c_{i'}c_{i''}}\right].$$

*Remark* 3.1. For $p \in \mathbb{N}$, let us consider the iterated function system

$$\mathcal{S}_p = ((X,d),(f_{i_1}\circ\cdots\circ f_{i_p})_{i_1,\dots,i_p\in\{1,\dots,n\}}).$$

Note that:

($\alpha$) (see Proposition 3.4 from [1]) $\mathcal{A}_{\mathcal{S}_p} = \mathcal{A}_{\mathcal{S}}$.

($\beta$) $d((f_{i_1}\circ\cdots\circ f_{i_p})(x),(f_{i_1}\circ\cdots\circ f_{i_p})(y)) \le c_{i_1}\cdot\ldots\cdot c_{i_p}d(x,y)$, for all $x,y\in X$ and $i_1,\dots,i_p\in\{1,\dots,n\}$.

Since $c_{i_1}\cdot\ldots\cdot c_{i_p} \le c_{i'}^p$, and $\lim_{p\to\infty} c_{i'}^p = 0$, via $\alpha$) and Theorem 3.1, we infer that, by increasing $p$, $\mathcal{A}_{\mathcal{S}}$ can be covered with a finite family of closed balls having the radii as small as we want.

### 3.2. Covers in the Particular Case of Fractal Interpolation Surfaces

In the sequel we shall consider a fractal interpolation surface, as introduced in Sect. 2.2.

**Lemma 3.1.** *For $k\in\{1,\dots,n\}$ and $l\in\{1,\dots,m\}$, $\gamma_{k,l} := (x_{k,l},y_{k,l},z_{k,l})$ is the unique fixed point of $F_{k,l}$, where $x_{k,l} = \frac{b_k}{1-a_k}$, $y_{k,l} = \frac{d_l}{1-c_l}$ and $z_{k,l} = \frac{1}{1-g_{k,l}}\left[e_{k,l}\frac{b_k}{1-a_k} + f_{k,l}\frac{d_l}{1-c_l} + \alpha_{k,l}\frac{b_kd_l}{(1-a_k)(1-c_l)} + \beta_{k,l}\right]$.*

*Proof.* For $k \in \{1,\dots,n\}$ and $l \in \{1,\dots,m\}$, let $\gamma_{k,l} = (x_{k,l}, y_{k,l}, z_{k,l})$ be the fixed point of $F_{k,l}$.

Then

$$\begin{cases} a_k x_{k,l} + b_k & = x_{k,l} \\ c_l y_{k,l} + d_l & = y_{k,l} \\ e_{k,l}x_{k,l} + f_{k,l}y_{k,l} + g_{k,l}z_{k,l} + \alpha_{k,l}x_{k,l}y_{k,l} + \beta_{k,l} & = z_{k,l} \end{cases}.$$

From the first two equation we deduce that

$$x_{k,l} = \frac{b_k}{1-a_k} \text{ and } y_{k,l} = \frac{d_l}{1-c_l}.$$

Substituting in the third equation we obtain

$$e_{k,l}\frac{b_k}{1-a_k} + f_{k,l}\frac{d_l}{1-c_l} + g_{k,l}z_{k,l} + \alpha_{k,l}\frac{b_k d_l}{(1-a_k)(1-c_l)} + \beta_{k,l} = z_{k,l}.$$

Therefore,

$$z_{k,l} = \frac{1}{1-g_{k,l}}\left[e_{k,l}\frac{b_k}{1-a_k} + f_{k,l}\frac{d_l}{1-c_l} + \alpha_{k,l}\frac{b_k d_l}{(1-a_k)(1-c_l)} + \beta_{k,l}\right].$$

□

*Remark* 3.2. The closed ball with respect to $\rho$, having radius $r > 0$ and center $(x_0, y_0, z_0) \in \mathbb{R}^3$, is the set $\{(x,y,z) \in \mathbb{R}^3 | \rho((x,y,z),(x_0,y_0,z_0)) \leq r\} = \{(x,y,z) \in \mathbb{R}^3 || x-x_0| + |y-y_0| + \theta|z-z_0| \leq r\}$, denoted by $O[(x_0,y_0,z_0), r]$.

This set is an octahedron having the following vertices: $V_1\,(x_0 + r, y_0, z_0)$, $V_2\,(x_0, y_0 + r, z_0)$, $V_3\left(x_0, y_0, z_0 + \frac{r}{\theta}\right)$, $V_4\,(x_0 - r, y_0, z_0)$, $V_5\,(x_0, y_0 - r, z_0)$ and $V_6\left(x_0, y_0, z_0 - \frac{r}{\theta}\right)$.

To summarize our previous results, we have identified the following quantities:

- $\delta := \max\{|a|, |b|, |c|, |d|\}$
- $\theta = \min\{\theta_1, \theta_2\}$, where

$$\theta_1 = \begin{cases} 1, & \begin{matrix} e_{1,1} = \cdots = e_{n,m} = 0 \\ \alpha_{1,1} = \cdots = \alpha_{n,m} = 0 \end{matrix} \\ \dfrac{1 - \max\limits_{k\in\{1,\dots,n\}} a_k}{2 \max\limits_{\substack{k\in\{1,\dots,n\} \\ l\in\{1,\dots,m\}}} (|e_{k,l}| + \delta|\alpha_{k,l}|)}, & \text{otherwise} \end{cases}$$

and

$$\theta_2 = \begin{cases} 1, & \begin{matrix} f_{1,1} = \cdots = f_{n,m} = 0 \\ \alpha_{1,1} = \cdots = \alpha_{n,m} = 0 \end{matrix} \\ \dfrac{1 - \max\limits_{l\in\{1,\dots,m\}} c_l}{2 \max\limits_{\substack{k\in\{1,\dots,n\} \\ l\in\{1,\dots,m\}}} (|f_{k,l}| + \delta|\alpha_{k,l}|)}, & \text{otherwise} \end{cases};$$

- $\gamma_{k,l} = (x_{k,l}, y_{k,l}, z_{k,l})$ with $x_{k,l} = \dfrac{b_k}{1-a_k}$, $y_{k,l} = \dfrac{d_l}{1-c_l}$,

$$z_{k,l}=\frac{1}{1-g_{k,l}}\left[e_{k,l}\frac{b_k}{1-a_k}+f_{k,l}\frac{d_l}{1-c_l}+\alpha_{k,l}\frac{b_kd_l}{(1-a_k)(1-c_l)}+\beta_{k,l}\right],$$

for all $k\in\{1,\dots,n\}$ and $l\in\{1,\dots,m\}$;

$\bullet C_{k,l}=\max\left\{a_k+\theta(|e_{k,l}|+\delta|\alpha_{k,l}|),\ c_l+\theta(|f_{k,l}|+\delta|\alpha_{k,l}|),g_{k,l}\right\},$

for all $k\in\{1,\dots,n\}$ and $l\in\{1,\dots,m\}$;

$\bullet M=\max\limits_{\substack{i,k\in\{1,\dots,n\}\\ j,l\in\{1,\dots,m\}}}\rho(\gamma_{i,j},\gamma_{k,l}).$

Let us choose $k',k''\in\{1,\dots,n\}$ and $l',l''\in\{1,\dots,m\}$ such that

$$C_{k',l'}=\max_{\substack{k\in\{1,\dots,n\}\\ l\in\{1,\dots,m\}}}C_{k,l}\qquad\text{and}\qquad C_{k'',l''}=\max_{\substack{k\in\{1,\dots,n\}\setminus\{k'\}\\ l\in\{1,\dots,m\}\setminus\{l'\}}}C_{k,l}.$$

Taking into account Theorem 3.1, with the notation $r'=\frac{1+C_{k',l'}}{1-C_{k',l'}C_{k'',l''}}$ and $r''=\frac{1+C_{k'',l''}}{1-C_{k',l'}C_{k'',l''}}$, we get

**Theorem 3.2.** *In this setting, the following inclusion holds*

$$G_f\subseteq\left(\bigcup_{\substack{k\in\{1,\dots,n\}\setminus\{k'\}\\ l\in\{1,\dots,m\}\setminus\{l'\}}}O\left[\gamma_{k,l},MC_{k,l}r'\right]\right)\bigcup O\left[\gamma_{k',l'},MC_{k',l'}r''\right].$$

The set

$$\left(\bigcup_{\substack{k\in\{1,\dots,n\}\setminus\{k'\}\\ l\in\{1,\dots,m\}\setminus\{l'\}}}O\left[\gamma_{k,l},MC_{k,l}r'\right]\right)\bigcup O\left[\gamma_{k',l'},MC_{k',l'}r''\right],$$

which is a cover of $\mathcal{A}_{\mathscr{S}}=G_f$, will be denoted by $\mathcal{C}_{\mathscr{S}}$.

For $p\in\mathbb{N}$, by $\mathcal{C}_p$ we designate $\mathcal{C}_{\mathscr{S}_p}$, which is also a cover of $G_f$.

*Remark* 3.3. In view of Remark 3.1, by increasing $p$, the diameters of the octahedrons occurring in $\mathcal{C}_p$ could be as small as we want.

### 3.3. Some Graphical Representations

We apply our results to the following data sets:

**Example 1.** Let

$$x_0=0,\ x_1=100,\ x_2=200,$$
$$y_0=0,\ y_1=100,\ y_2=200,$$

with the corresponding $z_{k,l}$ values

| $l$ \ $k$ | 0 | 1 | 2 |
|---|---|---|---|
| 0 | 0 | -10 | -20 |
| 1 | 10 | -30 | -10 |
| 2 | 20 | 10 | 0 |

and $g_{k,l}$ given by

| $l$ \ $k$ | 1 | 2 |
|---|---|---|
| 1 | 0.7 | 0.5 |
| 2 | 0.6 | 0.6 |

.

The interpolation surface obtained has the following graphical representation:

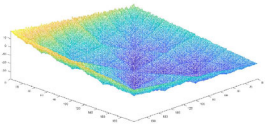

$(O)$ : Visualization of the graph of the interpolated surface

The figures $(I)$, $(II)$, $(III)$, $(IV)$, $(V)$ contain graphical representations of the covers $\mathcal{C}_1$, $\mathcal{C}_3$, $\mathcal{C}_5$, $\mathcal{C}_7$ and $\mathcal{C}_9$.

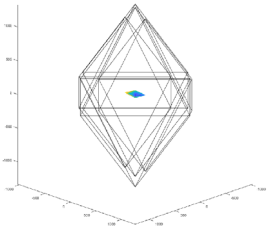

(I): Visualization of $\mathcal{C}_1$

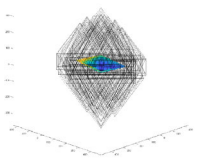

(II): Visualization of $\mathcal{C}_3$

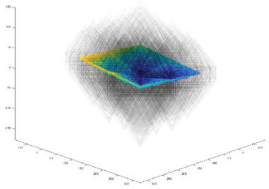

(III): Visualization of $\mathcal{C}_5$

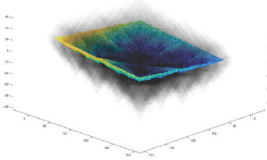

(IV): Visualization of $\mathcal{C}_7$

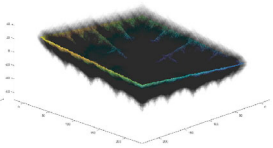

(V): Visualization of $\mathcal{C}_9$

**Example 2.** Let

$$x_0 = 0,\ x_1 = 100,\ x_2 = 200,\ x_3 = 300$$
$$y_0 = 0,\ y_1 = 100,\ y_2 = 200,\ y_3 = 300$$

with the corresponding $z_{k,l}$ values

| $l$ \ $k$ | 0 | 1 | 2 | 3 |
|---|---|---|---|---|
| 0 | 0 | 15 | 30 | 45 |
| 1 | -10 | 20 | -30 | 35 |
| 2 | -20 | 30 | 10 | 25 |
| 3 | -30 | -15 | 0 | 15 |

and $g_{k,l}$ given by

| $l$ \ $k$ | 1 | 2 | 3 |
|---|---|---|---|
| 1 | 0.3 | 0.2 | 0.5 |
| 2 | 0.4 | 0.7 | 0.6 |
| 3 | 0.3 | 0.6 | 0.4 |

.

The interpolation surface has the following graphical representation:

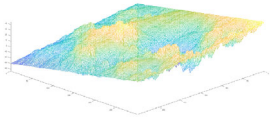

$(O)$ : Visualization of the graph of the interpolated surface

The figures $(I)$, $(II)$, $(III)$, $(IV)$, $(V)$ contain graphical representations of the covers $\mathcal{C}_1$, $\mathcal{C}_2$, $\mathcal{C}_3$, $\mathcal{C}_4$ and $\mathcal{C}_5$.

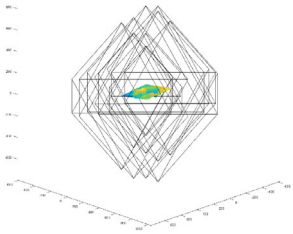

(I):Visualization of $\mathcal{C}_1$

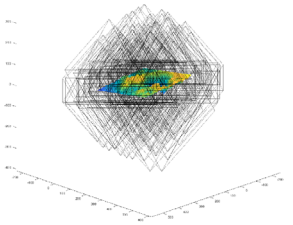

(II):Visualization of $\mathcal{C}_2$

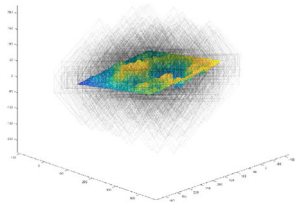

(III):Visualization of $\mathcal{C}_3$

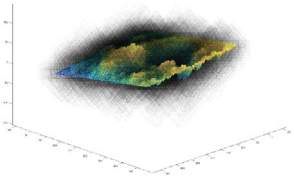

(IV):Visualization of $\mathcal{C}_4$

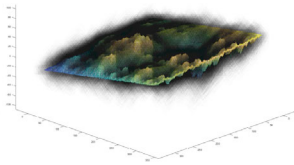

(V):Visualization of $\mathcal{C}_5$

**Acknowledgements**

We sincerely express our gratitude to the editors and the reviewers for the valuable feedback that has contributed to the improvement of this paper.

**Author contributions** Conceptualization, methodology and analysis, B.C.A. and R. M.; writing-review and editing B.C. A. and R. M.; proofreading and editing B.C.A. and R. M. All authors have read and agreed to the published version of the manuscript.

**Funding** Not applicable.

**Data Availability Statement** Not applicable.

**Declarations**

**Conflict of interest** The authors have no conflict of interest, or other interests that might be perceived to influence the results and/or discussions reported in this paper.



## Appendix

We provide the following functions, which were used to determine the covers presented in the previous examples.

**Input:** $x = [x_0, \ldots, x_n]$, $y = [y_0, \ldots, y_m]$, $z = \begin{bmatrix} z_{0,0}, \ldots, z_{0,m} \\ \vdots \quad\quad \vdots \\ z_{n,0}, \ldots, z_{n,m} \end{bmatrix}$, $g = \begin{bmatrix} g_{1,1}, \ldots, g_{1,m} \\ \vdots \quad\quad \vdots \\ g_{n,1}, \ldots, g_{n,m} \end{bmatrix}$.

**function** `coeff`($x$, $y$, $z$, $g$)**:**
- **for** $i \leftarrow 1$ **to** $n$ **do**
  - $F(i,j)(1) \leftarrow \frac{x(i)-x(i-1)}{x(n)-x(0)}$;
  - $F(i,j)(2) \leftarrow \frac{x(i)*x(n)-x(i-1)*x(0)}{x(n)-x(0)}$;
  - **for** $j \leftarrow 1$ **to** $m$ **do**
    - $p = z(i,j) - g(i,j)z(n,m); q = z(i-1,j) - g(i,j)z(0,m)$;
    - $r = z(i,j-1) - g(i,j)z(n,0); t = z(i-1,j-1) - g(i,j)z(0,0)$;
    - $F(i,j)(3) \leftarrow \frac{y(j)-y(j-1)}{y(n)-y(0)}$;
    - $F(i,j)(4) \leftarrow \frac{y(j)y(n)-y(j-1)y(0)}{y(n)-y(0)}$;
    - $F(i,j)(5) \leftarrow \frac{y(0)(q-p)-y(m)(t-r)}{(x(n)-x(0))(y(m)-y(0))}$;
    - $F(i,j)(6) \leftarrow \frac{x(0)(r-p)-x(n)(t-q)}{(x(n)-x(0))(y(m)-y(0))}$;
    - $F(i,j)(7) \leftarrow g(i,j)$;
    - $F(i,j)(8) \leftarrow \frac{p-q-r+t}{(x(n)-x(0))(y(m)-y(0))}$;
    - $F(i,j)(9) \leftarrow \frac{y(0)(x(0)p-x(n)q)-y(m)(x(0)r-x(n)t)}{(x(n)-x(0))(y(m)-y(0))}$;
- **return** $F$;

**function** `theta`($F$, $\delta$)**:**
- **for** $i \leftarrow 1$ **to** $n$ *and* $j \leftarrow 1$ **to** $m$ **do**
  - $[a,b,c,d,e,f,g,\alpha,\beta] \leftarrow$ F(i, j);
  - $max_a \leftarrow \max(max_a, a)$; $max_c \leftarrow \max(max_c, c)$;
  - $max_1 \leftarrow \max(max_1, |e| + \delta|\alpha|)$; $max_2 \leftarrow \max(max_2, |f| + \delta|\alpha|)$;
- $\theta_1 = \theta_2 = 1$
- **if** $max_1 \neq 0$ **then**
  - $\theta_1 \leftarrow \frac{1-max_a}{2*max_1}$
- **if** $max_2 \neq 0$ **then**
  - $\theta_2 \leftarrow \frac{1-max_c}{2*max_2}$
- $\theta = \min(\theta_1, \theta_2)$;
- **return** $\theta$;

**function** `fixPT`($F$)**:**
- **for** $i \leftarrow 1$ **to** $n$ *and* $j \leftarrow 1$ **to** $m$ **do**
  - $[a,b,c,d,e,f,g,\alpha,\beta] \leftarrow F(i,j)$;
  - $\gamma(i,j) \leftarrow [\frac{b}{1-a}, \frac{d}{1-c}, \frac{1}{1-g(i,j)}\left(\frac{eb}{1-a} + \frac{fd}{1-c} + \frac{\alpha bd}{(1-a)*(1-c)} + \beta\right)]$;
- **return** $\gamma$;

**function** `const`($F$, $\theta$)**:**
- **for** $i \leftarrow 1$ **to** $n$ *and* $j \leftarrow 1$ **to** $m$ **do**
  - $[a,b,c,d,e,\alpha,\beta] \leftarrow F(i,j)$;
  - $c(i,j) \leftarrow \max(a + \theta(|e| + \delta|\alpha|), c + \theta(|f| + \delta|\alpha|), g(i,j)))$;
- **return** $\theta$;

**function** `radii`($k$, $l$, $c$, $M$)**:**
- $max_c \leftarrow [0,0]$; $ind_1 \leftarrow [0,0]$; $ind_2 \leftarrow [0,0]$;
- **for** $i \leftarrow 1$ **to** $k$ *and* $j \leftarrow 1$ **to** $l$ **do**
  - **if** $max_c(1) \leq c(i,j)$ **then**
    - $max_c(2) \leftarrow max_c(1)$; $ind_2 \leftarrow ind_1$;
    - $max_c(1) \leftarrow c(i,j)$; $ind_1 \leftarrow [i,j]$;
- $r(ind_1) \leftarrow c(ind_1) * M * (1 + c(ind_2))/(1 - c(ind_2) * c(ind_1))$;
- **for** $i \leftarrow 1$ **to** $k$ *and* $j \leftarrow 1$ **to** $l$, $[i,j] \neq ind_1$ **do**
  - $r(i,j) \leftarrow c(i,j) * M * (1 + c(ind_1))/(1 - c(ind_2) * c(ind_1))$;
- **return** $r$;

**function** `vertices`($k$, $l$, $\gamma$, $r$, $\theta$)**:**
- **for** $i \leftarrow 1$ **to** $k$ *and* $j \leftarrow 1$ **to** $l$ **do**
  - $O(i,j) \leftarrow [\gamma(i,j) + [r(i,j), 0, 0], \gamma(i,j) - [r(i,j), 0, 0],$
    $\gamma(i,j) + [0, r(i,j), 0], \gamma(i,j) - [0, r(i,j), 0],$
    $\gamma(i,j) + [0, 0, r(i,j)/\theta], \gamma(i,j) - [0, 0, r(i,j)/\theta]]$;
- **return** $O$;

`/*` $r$ `contains the radii and` $O$ `is a matrix in which each element` $o_{i,j}$ `contains the eight vertices that define the octahedron corresponding to each function in the system.` `*/`

To calculate the composition's coefficients one can use the following functions:

**Input:** $F_0 = \begin{bmatrix} F_{1,1}, \ldots, F_{1,m} \\ \vdots \quad\quad \vdots \\ F_{n,1}, \ldots, F_{n,m} \end{bmatrix}$, $c_0 = \begin{bmatrix} c_{1,1}, \ldots, c_{1,m} \\ \vdots \quad\quad \vdots \\ c_{n,1}, \ldots, c_{n,m}. \end{bmatrix}$, $order$

**Output:** $F_n, c_n$

**function** `comp2`$([a_1, b_1, c_1, d_1, e_1, f_1, g_1, \alpha_1, \beta_1],\ [a_2, b_2, c_2, d_2, e_2, f_2, g_2, \alpha_2, \beta_2])$**:**

- $a \leftarrow a_1 * a_2$;
- $b \leftarrow a_1 * b_2 + b_1$;
- $c \leftarrow c_1 * c_2$;
- $d \leftarrow c_1 * d_2 + d_1$;
- $e \leftarrow e_1 * a_2 + g_1 * e_2 + \alpha_1 * a_2 * d_2$;
- $f \leftarrow f_1 * c_2 + g_1 * f_2 + \alpha_1 * b_2 * c_2$;
- $g \leftarrow g_1 * g_2$;
- $\alpha \leftarrow \alpha_1 * a_2 * c_2 + g_1 * \alpha_2$;
- $\beta \leftarrow e_1 * b_2 + f_1 * d_2 + \alpha_1 * b_2 * d_2 + g_1 * \beta_2 + \beta_1$;
- **return** $[a, b, c, d, e, f, g, \alpha, \beta]$;

**function** `sisComp`$(F_o,\ F_n,\ c_o,\ c_n)$**:**

- $index_1 \leftarrow 0$;
- **for** $i \leftarrow 1$ **to** $n$ *and* $j \leftarrow 1$ **to** $m$ **do**
  - $index_1 \leftarrow index_1 + 1$;
  - $index_2 \leftarrow 0$;
  - **for** $k \leftarrow 1$ **to** $n'$ *and* $l \leftarrow 1$ **to** $m'$ **do**
    - $index_2 \leftarrow index_2 + 1$;
    - $F(index_1, index_2) = comp2(F_o(i, j), F_n(k, l))$;
    - $c(index_1, index_2) = c_o(i, j) * c_n(k, l)$;
- **return** $F, c$;

**function** `sisCompOrd`$(F_o, c_o, order)$**:**

- **if** $order \geq 2$ **then**
  - $[F_n, c_n] \leftarrow$sisComp$(F_o, F_o, c_o, c_o)$;
  - **for** $i \leftarrow 3$ **to** $order$ **do**
    - $[F_n, c_n] \leftarrow$sisComp$(F_o, F_n, c_o, c_n)$;
- **else**
  - **return** $F_o, c_o$;
- **return** $F_n, c_n$;

## References


[1] Anghelina, B., Miculescu, R.: On the localization of Hutchinson–Barnsley fractals. Chaos Solitons Fract. **173**, 113674 (2023)

[2] Barnsley, M.: Fractal functions and interpolation. Constr. Approx. **2**, 303–329 (1986)

[3] Barnsley, M., Elton, J., Hardin, D., Massopust, P.: Hidden variable fractal interpolation functions. SIAM J. Math. Anal. **20**, 1218–1242 (1998)

[4] Barnsley, M., Viswanathan, P.: Histopolating fractal functions. J. Comput. Appl. Math **425**, 115073 (2023)

[5] Bouboulis, P., Dalla, L.: Closed fractal interpolation surfaces. J. Math. Anal. Appl. **327**, 116–126 (2007)

[6] Bouboulis, P., Dalla, L.: Fractal interpolation surfaces derived from fractal interpolation functions. J. Math. Anal. Appl. **336**, 919–936 (2007)

[7] Bouboulis, P., Dalla, L., Drakopoulos, V.: Image compression using recurrent bivariate fractal interpolation surfaces. Int. J. Bifurcat. Chaos **16**, 2063–2071 (2006)

[8] Cambell, B., Shepard, M.: Shadows on a planetary surface and implications for photometric roughness. ICARUS **134**, 279–291 (1998)

[9] Chand, A.K.B., Vijender, N.: A new class of fractal interpolation surfaces based on functional values. Fractals **24**, 1650007 (2016)

[10] Chand, A.K.B., Tyada, K.: Partially blended constrained rational cubic trigonometric fractal interpolation surfaces. Fractals **24**, 1650027 (2016)

[11] Dalla, L.: Bivariate fractal interpolation functions on grids. Fractals **10**, 53–58 (2002)

[12] Drakopoulos, V., Manousopoulos, P.: Bivariate fractal interpolation surfaces: theory and applications. Int. J. Bifurcat. Chaos Appl. Sci. Eng. **22**, 1250220 (2012)

[13] Feng, Z.: Variation and Minkowski dimension of fractal interpolation surface. J. Math. Anal. Appl. **345**, 322–334 (2008)

[14] Feng, Z., Feng, Y., Yuan, Z.: Fractal interpolation surfaces with function vertical scaling factors. Appl. Math. Lett. **25**, 1896–1900 (2012)

[15] Geronimo, J., Hardin, D.: Fractal interpolation surfaces and a related 2D multiresolution analysis. J. Math. Anal. Appl. **176**, 346–355 (1993)

[16] Hardin, D., Massopust, P.: Fractal interpolation functions from $\mathbb{R}^n \to \mathbb{R}^m$ and their projections. Z. Anal. Anw. **12**, 535–548 (1993)

[17] Hutchinson, J.: Fractals and self similarity. Indiana Univ. Math. J. **30**, 713–747 (1981)

[18] Lal, R., Chandra, S., Prajapati, A.: Fractal surfaces in Lebesgue spaces with respect to fractal measures and associated fractal operators. Chaos Solitons Fract. **181**, 114684 (2024)

[19] Liang, Z., Ruan, H.: Recurrent fractal interpolation surfaces on triangular domains. Fractals **27**, 1950085 (2019)

[20] Liang, Z., Ruan, H.: Construction and box dimension of recurrent fractal interpolation surfaces. J. Fractal Geom. **8**, 261–288 (2021)

[21] Małysz, R.: The Minkowski dimension of the bivariate fractal interpolation surfaces. Chaos Solitons Fract. **27**, 1147–1156 (2006)

[22] Massopust, P.: Fractal surfaces. J. Math. Anal. Appl. **151**, 275–290 (1990)

[23] Metzler, W., Yun, C.: Construction of fractal interpolation surfaces on rectangular grids. Int. J. Bifurcat. Chaos **20**, 4079–4086 (2010)

[24] Pandey, K., Secelean, N., Viswanathan, P.: On bivariate fractal interpolation for countable data and associated nonlinear fractal operator. Demonstr. Math. **57**, 20240014 (2024)

[25] Ri, S.: A new construction of the fractal interpolation surface. Fractals **23**, 1550043 (2015)

[26] Ri, S.: New types of fractal interpolation surfaces. Chaos Solitons Fract. **123**, 52–58 (2019)

[27] Ri, S., Drakopoulos, V.: Generalised fractal interpolation curved lines and surfaces. Nonlinear Stud. **28**, 427–488 (2021)

[28] Ruan, H., Xu, Q.: Fractal interpolation surfaces on rectangular grids. Bull. Aust. Math. Soc. **91**, 435–446 (2015)

[29] Verma, S., Viswanathan, P.: A fractal operator associated with bivariate fractal interpolation functions on rectangular grids. Results Math. **75**, 28 (2020)

[30] Vijay, Chand, A.K.B.: Convexity-preserving rational cubic zipper fractal interpolation curves and surfaces. Math. Comput. Appl. **28**, 74 (2023)

[31] Vijay, Chand, A.K.B.: $C^1$-Positivity preserving bi-quintic blended rational quartic zipper fractal interpolation surfaces. Chaos Solitons Fract. **188**, 115472 (2024)

[32] Xie, H., Sun, H.: The study of bivariate fractal interpolation functions and creation of fractal interpolated surfaces. Fractals **5**, 625–634 (1997)

[33] Xie, H., Sun, H., Zu, Y., Feng, Z.: Study on generation of rock fracture surfaces by using fractal interpolation. Int. J. Solids Struct. **38**, 5765–5787 (2001)

[34] Yokoya, N., Yamamoto, K., Funakubo, N.: Fractal-based analysis and interpolation of 3D natural surface shapes and their application to terrain modeling. Comput. Vis. Graph. Image Process **46**, 284–302 (1989)

[35] Yun, C., O, H., Choi, H.: Construction of fractal surfaces by recurrent fractal interpolation curves. Chaos Solitons Fract. **66**, 136–143 (2014)

[36] Zhao, N.: Construction and application of fractal interpolation surfaces. Vis. Comput. **12**, 132–146 (1996)

Bogdan-Cristian Anghelina and Radu Miculescu
Faculty of Mathematics and Computer Science
Transilvania University of Brașov
Iuliu Maniu Street, nr. 50
500091 Brașov
Romania
e-mail: radu.miculescu@unitbv.ro

Bogdan-Cristian Anghelina
e-mail: bogdan.anghelina@unitbv.ro

Received: October 22, 2024.

Revised: March 2, 2025.

Accepted: March 29, 2025.